Modification of the SDR equation for permeability prediction

Andreas Weller[1,*], and *Zeyu* Zhang[1]

[1]Technische Universität Clausthal, Institut für Geophysik, 38678 Clausthal-Zellerfeld, Germany

Abstract. We evaluate the potential of permeability prediction of the original and modified versions of the Schlumberger-Doll Research (SDR) equation that is applied to data of nuclear magnetic resonance (NMR) relaxometry. Different definitions of characteristic relaxation time are considered. In a further modification, pore radius replaces the characteristic relaxation time in the original SDR equation. Only a good estimate of the surface relaxivity enables a reliable transformation from the relaxation time distribution (RTD) into the pore radius distribution (PRD). A recently published approach considers the specific surface area per unit pore volume (S_{por}) and the weighted harmonic mean (T_{2hm}) of the RTD for the determination of an individual value of surface relaxivity for each sample. The evaluation is performed for three sample sets originating from different sandstone formations. The good predictive quality of the original SDR equation is confirmed. However, the prefactors have to be adjusted by calibrating with core data. We demonstrate that the use of average pore radii instead of average relaxation times enables a better permeability prediction. The weighted harmonic mean of the PRD, which proves to be a reliable proxy for the effective hydraulic radius, provides a high quality permeability prediction.

1 Introduction

Permeability prediction for reservoir rocks is still a challenge in geophysical exploration. Porosity and pore radius are the most relevant parameters used in models of permeability prediction. A variety of petrophysical experiments or logging tools provide reliable porosity values. The effective hydraulic radius r_{eff} controls the fluid flow through porous rocks with a certain pore radius distribution (PRD).

Nuclear magnetic resonance (NMR) relaxometry provides an estimate of porosity and a relaxation time distribution (RTD). The maximum or mean values of the RTD are regarded as proxies for the effective hydraulic radius. The original Schlumberger-Doll Research (SDR) equation relates the weighted geometric mean of the transverse relaxation time and porosity to permeability. In the common form of SDR equation, the relaxation time is raised to the 2nd power and porosity to the 4th power.

Using NMR data of samples originating from three sandstone formations, we investigate the relationships between different characteristic relaxation times and r_{eff}. In a further step, we evaluate the predictive quality of the original and modified SDR equations.

The transformation of characteristic relaxation times into characteristic pore radii requires the knowledge of the surface relaxivity [1]. Using the procedure of [2], we determine an individual value of surface relaxivity for each sample. We investigate whether the different characteristic pore radii can be used as suitable proxies for r_{eff}. In a further modification of the SDR equation, we replace the characteristic relaxation time by a characteristic pore radius. We demonstrate that this substantial modification enables an improvement of permeability prediction.

2 Theory

Numerous theoretical approaches for permeability estimation of porous rocks have been presented. They link parameters of pore space geometry to permeability. A simple model, which considers the fluid flow through capillary bundles with uniform pore radius, relates permeability to the pore radius r and the resistivity formation factor F (e.g., [3, 4]):

$$k = r^2/(8F). \quad (1)$$

Using the first Archie equation [5], which describes the relationship between F and porosity ϕ:

$$F = \frac{1}{\phi^m}, \quad (2)$$

where m is the cementation exponent, we get a permeability prediction model that considers the two parameters pore radius r and porosity ϕ:

$$k = \frac{1}{8}\phi^m r^2. \quad (3)$$

The porosity exponent m proves to be variable. For straight and parallel capillaries, an exponent $m = 1$ should be selected, whereas $m = 2$ is a good choice for consolidated sandstones. Larger exponents m are found especially for vuggy reservoir rocks (e.g., [6, 7]). Considering the physical dimensions of k (in m²) and r (in m), the exponent of r seems to be fixed at two. A more general form of equation 3 reads

$$k = a\phi^b r^2, \quad (4)$$

with two adjustable parameters: the prefactor a and the porosity exponent b. Equation 4 suggests that the quality of

* Corresponding author: andreas.weller@tu-clausthal.de

permeability prediction depends on reliable values of porosity and pore radius. There are several procedures applicable in the laboratory or in well logging that provide good estimates of porosity. Considering the wide variation of pore radii in porous rocks, the determination of the relevant characteristic pore radius is challenging.

The application of equation 4 requires a good proxy for the pore radius *r*. Regarding equation 1, the effective hydraulic radius

$$r_{eff} = \sqrt{8Fk} \tag{5}$$

can be determined for rock samples with known values of *F* and *k*. In this study, we use the effective hydraulic radius concept [8] to evaluate the predictive quality of proxies of the pore radius in equation 4.

The NMR method records the decay of magnetization after an excitation impulse has changed the magnetic orientation of the hydrogen nuclei. The measured transverse decay curve is transformed in a discrete distribution of relaxation times $b_i(T_{2i})$, where the index *i* is the sequential number of the predefined relaxation time T_2, and b_i is the resulting normalized amplitude. The normalization considers that the sum of all individual b_i equals one [2].

The Schlumberger-Doll Research (SDR) equation for permeability prediction from NMR relaxometry reads (e.g., [9]):

$$k^* = a_1\, \phi^4\, \overline{T_2}^2, \tag{6}$$

where k^* is the predicted permeability and $\overline{T_2}$ a characteristic relaxation time that is determined from the transverse relaxation time distribution. The empirical coefficient a_1 is adjusted for lithology by calibrating with core data. Equation 6 corresponds to the general form of equation 4 with the porosity exponent $b = 4$. The characteristic relaxation time $\overline{T_2}$ is used as a proxy for the pore radius. Different characteristic values are determined from the relaxation time distribution $b_i(T_{2i})$. The original form of the SDR equation applies the weighted geometric mean as a characteristic relaxation time:

$$T_{2lm} = \exp(\textstyle\sum_{i=1}^{n} b_i \ln T_{2i}). \tag{7}$$

Since the geometric mean uses a weighting of the logarithms of T_2, several authors use the name log-mean (e.g., [9]). We adopt this term and use the standard subscript *lm* for this weighted mean value. Other characteristic values are the weighted harmonic mean T_{2hm} that is calculated by

$$T_{2hm} = \frac{1}{\sum_{i=1}^{n} \frac{b_i}{T_{2i}}}, \tag{8}$$

or the weighted arithmetic mean

$$T_{2am} = \textstyle\sum_{i}^{n} b_i T_{2i}. \tag{9}$$

T_{2peak} is another characteristic relaxation time $\overline{T_2}$ that corresponds to the maximum of the relaxation time distribution.

We evaluate the relationships between different characteristic relaxation times $\overline{T_2}$ and r_{eff} for selected sample sets in order to identify the most suitable characteristic relaxation time. The prefactors a_1 in equation 6 are adjusted for the individual sample sets.

It has been shown in a variety of studies (e.g., [9, 10]) that a linear relationship between a characteristic pore radius $\bar{r}$ and characteristic relaxation time $\overline{T_2}$ can be assumed:

$$\bar{r} = 2\rho\overline{T_2}, \tag{10}$$

where ρ is the transverse surface relaxivity. We use the approach of [2] to determine an individual value of surface relaxivity for each sample:

$$\rho = \left[S_{por} \times \left(\frac{2\,T_{2min}}{\lambda_2}\right)^{(D_t - D_f)} \times T_{2hm}\right]^{\left(\frac{-1}{1+D_t-D_f}\right)}, \tag{11}$$

where D_f is the fractal dimension and $D_t = 2$ the topological dimension of the pore surface area. The specific surface area per unit pore volume S_{por} is determined from the nitrogen adsorption method with the resolution $\lambda_2 = 0.4$ nm.

Using equation 10 with different characteristic relaxation times and the individual values of surface relaxivity of each sample, we get the weighted characteristic pore radii r_{lm}, r_{hm}, and r_{am}. T_{2peak} is converted into r_{dom} in the same way. We investigate whether the resulting characteristic pore radii are suitable proxies for r_{eff}.

3 Samples and methods

The evaluation of the original and modified versions of the SDR equation is based on data from three different sandstone formations:

1) The first set of samples originates from the Shahejie Formation in the Dongpu Depression, Wenliu Oilfield, being located in the Northeast of Henan Province, China, between latitudes N 35° and N 36° and longitudes E 114°30′ and E115°30′. The geological age of this formation is Eocene Epoch, Paleogene Period (approx. 35-56 Ma old). The samples have been collected in six boreholes in the depth interval between 3332 m and 3738 m. This set of 24 samples was used in studies related to permeability prediction, which were reported in [2] and [11].

2) The second set of samples was collected from the outcrops of Araba Formation in Wadi Saal, east central Sinai, Egypt, between latitude N 29° and N 30° and longitude E 34° and E 35°. This formation is of Carboniferous age or older (Lower Paleozoic). Considering the weak clay content, most of the investigated samples can be classified as clean sandstones. Petrographically, the 14 sandstone samples of the studied Araba Formation can be classified into three facies associations: (i) quartz arenite, (ii) sublithic quartz arenite, and (iii) calcareous quartz arenite. These facies are characterized by the presence of some pyrite and iron oxides as cement [12].

3) The third set, which consists of 20 samples, originates from the Cretaceous Nubia Formation, which reaches an approximate thickness of 40 m. Samples were taken in Wadi Ras El-Esh in the Red Sea area of Eastern Desert, Egypt, at longitude N 27° 27 ′58 ″ and latitude E 33° 30′ 51″. These sandstone beds are yellowish, highly dissected, cross-bedded, and rarely fossiliferous. The sandstone samples were differentiated into five microfacies

associations: quartz arenite, lithic quartz arenite, calcareous quartz arenite, quartz wacke, and gypsum quartz arenite. This formation includes both clean and clay-cemented sandstones.

The sample sets of the Araba and Nubia Formations have been integrated in a previous study on permeability prediction that is published in [13].

Cylindrical plugs with a diameter of about 25 mm and a length of about 30 mm have been prepared from all samples. This plug size is suitable for the required petrophysical experiments. Gas permeability k is determined in a steady state flow experiment following the guidelines of [14]. The resistivity formation factor F was measured in an electrical experiment with the plugs saturated with a high salinity brine (~ 15 S/m). The specific surface area per unit mass was determined by nitrogen adsorption method.

The NMR experiments were performed on the MARAN 7 instrument that is operating at a Lamor frequency of 7 MHz. The samples were saturated with a low salinity brine (~ 0.5 g/l NaCl) before the measurements. The signal decay curve, which was measured in the transverse mode, was transformed into a relaxation time distribution (RTD) using a least-squares algorithm that minimizes the deviation between measured and calculated curves. The weighted mean values T_{lm}, T_{hm}, and T_{am} of the RTD consider the interval between $T_{2min} = \tau_{echo} = 0.6$ ms and $T_{2max} = 3$ s.

4 Results

The relationships between characteristic relaxation times and r_{eff} are compared for the three sandstone formations in double logarithmic plots as shown in Figures 1 and 2 for T_{lm} and T_{hm}, respectively. A power law fitting was performed for each sample set. The resulting equations and the coefficient of determination (R^2) are displayed in the legend.

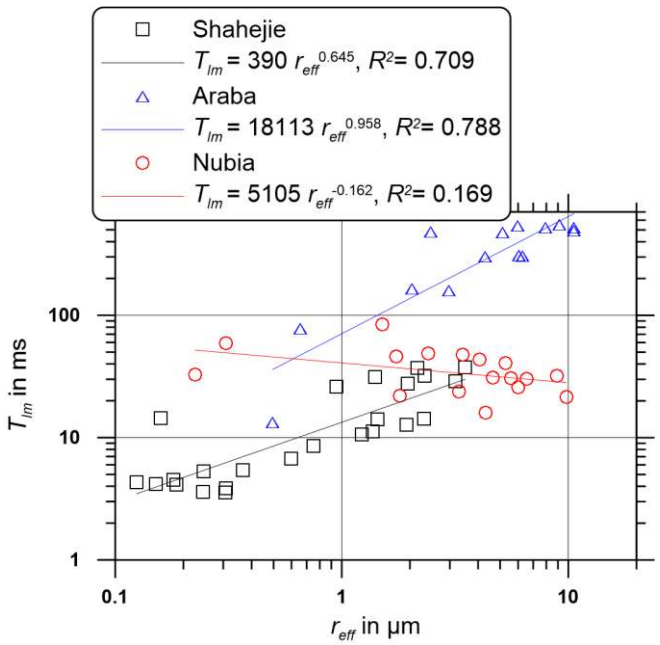

Fig. 1. Relationships between r_{eff} and T_{lm} for three sandstone formations.

The relationships between the logarithm of r_{eff} and the logarithm of the characteristic pore radii r_{lm} and r_{hm} are shown in Figure 3 and 4, respectively. The fitting equation assumes a linear relationship between the characteristic pore radius and r_{eff}.

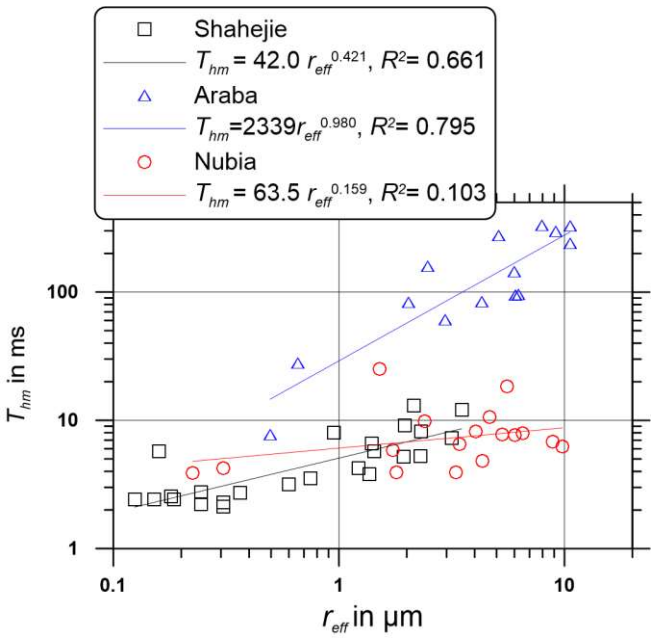

Fig. 2. Relationships between r_{eff} with T_{hm} for three sandstone formations.

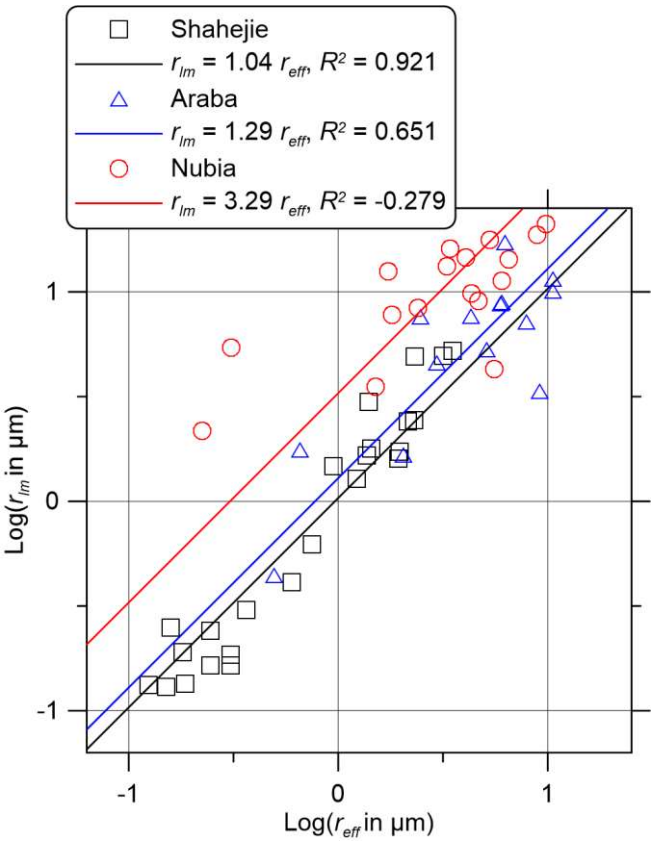

Fig. 3. Relationship between r_{eff} and characteristic pore radii r_{lm} for three sandstone formations.

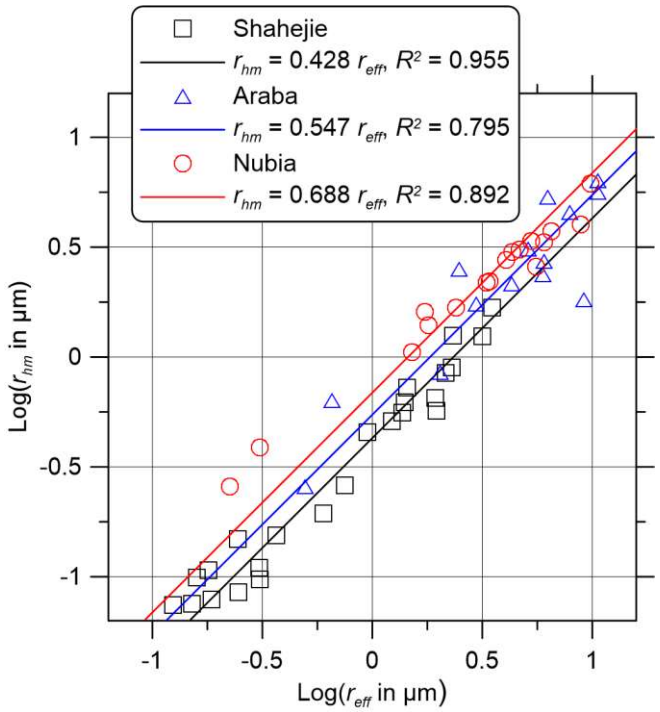

Fig. 4. Relationship between r_{eff} and characteristic pore radii r_{hm} for three sandstone formations.

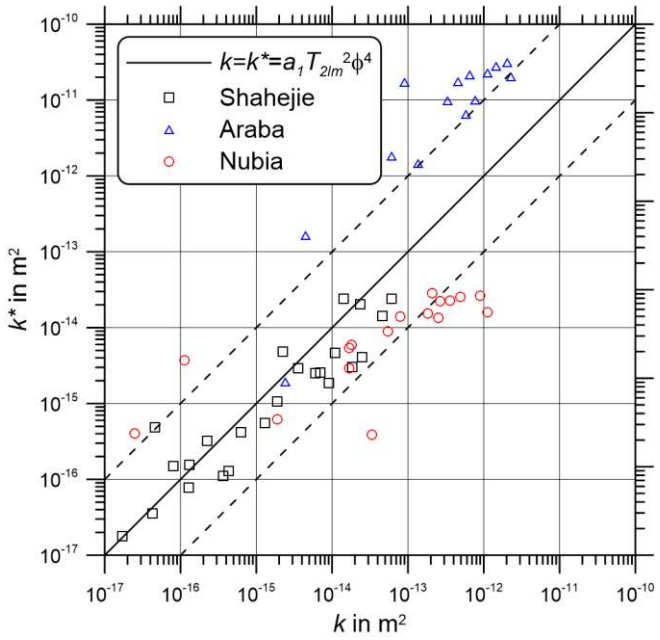

Fig. 5. Comparison of measured permeability k with $k^*=a_1 T_{2lm}^2 \phi^4$ (original SDR equation 6) for three sandstone formations. A uniform prefactor a_1 = 24.4·10^{-9} m²/s² has been determined considering the samples of the three formations The two dashed lines on either side of the diagonal indicate a deviation of one order of magnitude from the measured permeability value.

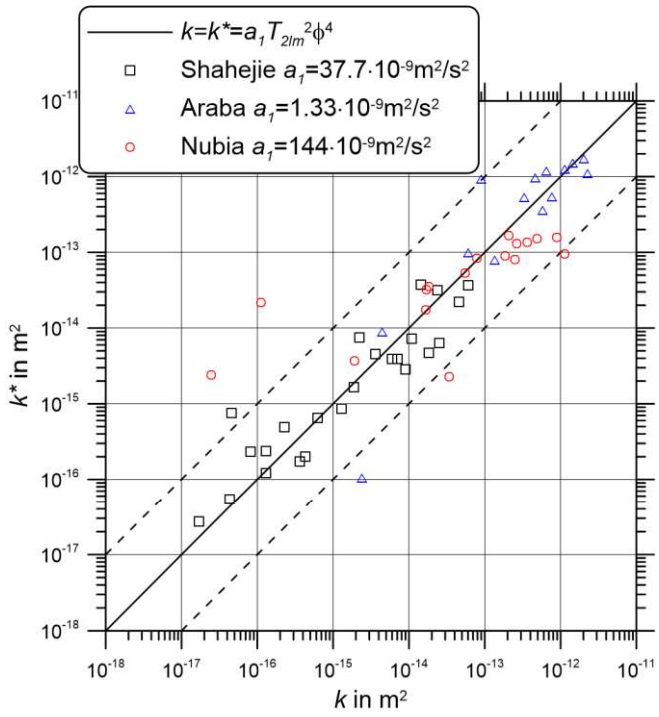

Fig. 6. Comparison of measured permeability k with $k^*=a_1 T_{2lm}^2 \phi^4$ (original SDR equation 6) for three sandstone formations. Individual prefactors a_1 have been determined for the three sandstone formations. The two dashed lines on either side of the diagonal indicate a deviation of one order of magnitude from the measured permeability value.

In order to evaluate the predictive quality of the original or modified SDR equations, we determine the average absolute deviation (in log space) between predicted permeability k^* and the measured permeability k (e.g., [15]):

$$d = \frac{1}{n} \sum_{j=1}^{n} \left| \log_{10}(k_j) - \log_{10}(k_j^*) \right|. \quad (12)$$

A value of d = 1 denotes an average absolute deviation of one order of magnitude (or a factor 10). One order of magnitude above or below the measured value is rated as an acceptable estimation if samples of different formations are regarded [16]. In the case of samples originating from the same formation, we aim at a better predictive quality with values considerably smaller than d = 0.5.

Figure 5 compares the measured permeability k with the permeability k^* predicted by the original SDR equation 6 with $\overline{T_2} = T_{2lm}$. A prefactor a_1 = 24.4·10^{-9} m²/s² has been determined considering all samples of the three formations in the adjustment procedure. We get a moderate agreement between measured and predicted permeability with d = 0.822.

The use of a separate adjustment procedure for each sandstone formation yields a better agreement d = 0.410 between measured and predicted permeability as demonstrated in Figure 6. The legend indicates the individual prefactors for the three sandstone formations that vary over two orders of magnitude.

Figure 7 displays the comparison between measured permeability k and the permeability k^* predicted by the SDR equation 6 using T_{2hm} instead of T_{2lm}. A uniform prefactor a_1 = 214.6·10^{-9} m²/s² has been determined using all samples

of this study. The deviation between measured and predicted permeability is $d = 0.936$.

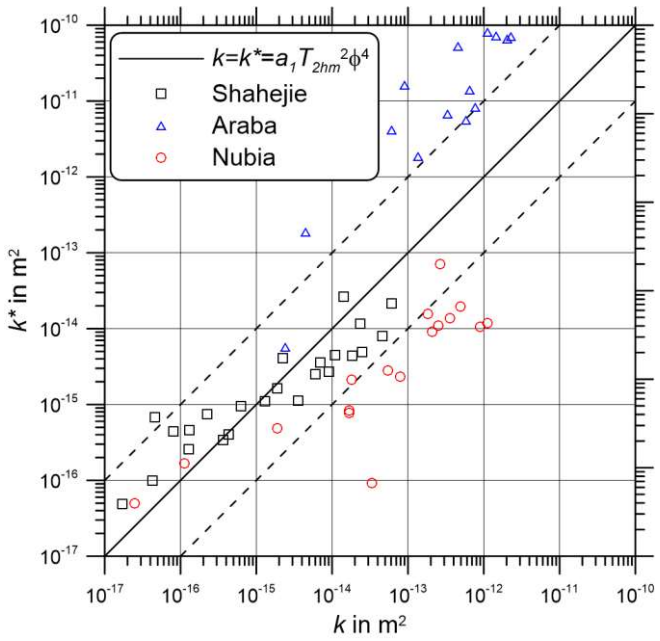

Fig. 7. Comparison of measured permeability k with $k^*=a_1 T_{2hm}^2 \phi^4$ (equation 6) for three sandstone formations. A uniform prefactor $a_1 = 214.6 \cdot 10^{-9}$ m²/s² has been determined considering the samples of the three formations The two dashed lines on either side of the diagonal indicate a deviation of one order of magnitude from the measured permeability value.

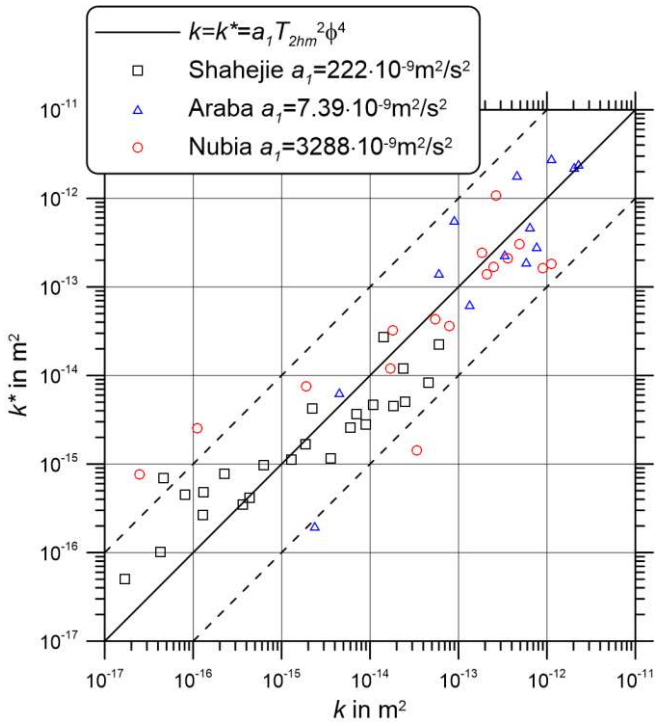

Fig. 8. Comparison of measured permeability k with $k^*=a_1 T_{2hm}^2 \phi^4$ (equation 6) for three sandstone formations. Individual prefactors a_1 have been determined for the three sandstone formations. The two dashed lines on either side of the diagonal indicate a deviation of one order of magnitude from the measured permeability value.

Figure 8 displays the comparison of measured permeability k and the permeability k^* predicted by the SDR equation using T_{2hm} instead of T_{2lm} with individual prefactors ($d = 0.435$).

The original SDR equation 6 considers a porosity exponent $b = 4$. Previous investigations have confirmed the suitability of this exponent. However, it is questionable whether the same exponent b should be used if characteristic pore radii replace the characteristic relaxations times. We investigate the predictive quality of equation 4 with different characteristic pore radii as proxies for r. The exponent b varies from 0 to 10. Figure 9 displays the average logarithmic deviation d as a function of the exponent b. The curves r_{am}, r_{lm} and r_{hm} indicate a minimum in the investigated range of the exponent b. We get the lowest average logarithmic deviation with $d = 0.211$ for the weighted harmonic mean r_{hm} and a porosity exponent $b = 2$.

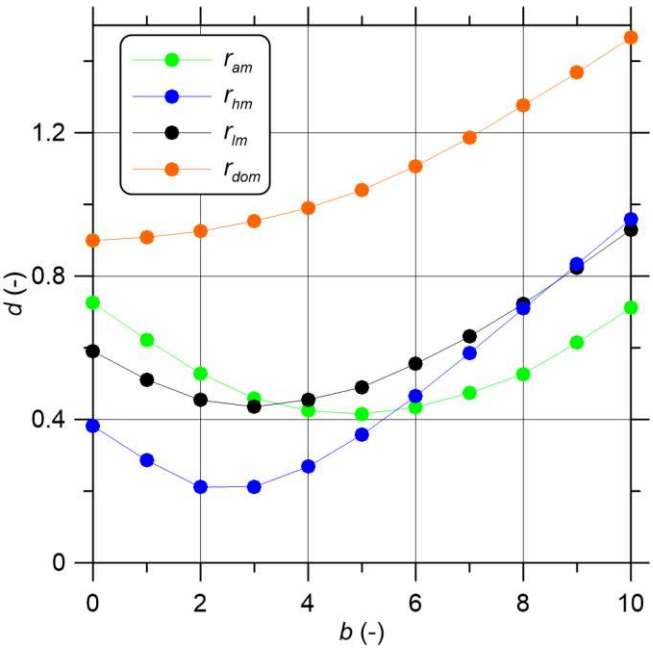

Fig. 9. Average logarithmic deviation d as function of the porosity exponent b in equation 4 using different characteristic pore radii $\bar{r}$ of the three sets of sandstone samples

Figure 10 shows the very good agreement between measured and predicted permeability for the model using the weighted harmonic mean of pore radius in equation 4.

The resulting prefactors a_1 of equation 6 (with $b = 4$) and the prefactors a of equation 4 (with $b = 2$) and the corresponding deviations d are compiled in Table 1.

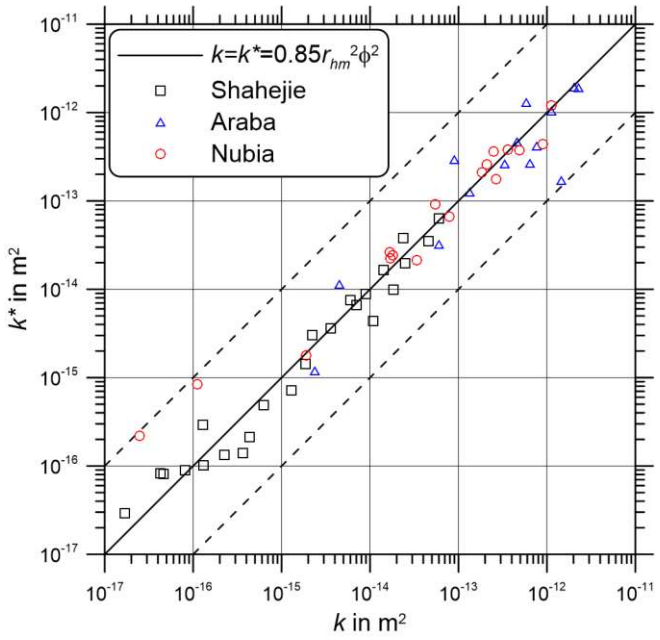

Fig. 10. Comparison of measured permeability k with $k^*=a\ r_{hm}^2\phi^2$ (equation 4) for three sandstone formations. A uniform prefactor $a = 0.85$ has been determined considering the samples of the three formations. The two dashed lines on either side of the diagonal indicate a deviation of one order of magnitude from the measured permeability value.

Table 1. The prefactors a_1 of equation 6 (in 10^{-9} m²/s²) and the prefactors a of equation 4 (dimensionless) with the resulting average deviations d (equation 12)

	Shahejie		Araba		Nubia		All samples	
Equation 6 (b = 4)	a_1	d	a_1	d	a_1	d	a_1	d
T_{2am}	3.11	0.443	0.54	0.323	17.3	0.769	3.38	0.745
T_{2hm}	221.56	0.411	7.39	0.373	3289	0.520	214.63	0.936
T_{2lm}	37.75	0.314	1.33	0.336	144.42	0.608	24.37	0.822
T_{2peak}	23.47	0.517	0.54	0.437	497.82	1.258	23.13	1.102
Equation 4 (b = 2)	a (-)	d	a (-)	d	a (-)	d	a (-)	d
r_{am}	0.01	0.222	0.08	0.445	0.003	0.675	0.01	0.528
r_{hm}	0.92	0.173	1.03	0.253	0.65	0.217	0.85	0.211
r_{lm}	0.16	0.280	0.18	0.401	0.03	0.488	0.10	0.454
r_{dom}	0.10	0.760	0.08	0.525	0.10	1.490	0.09	0.925

5 Discussion

Various models of permeability prediction require porosity and average pore radius as input parameters. The porosity can be derived either from NMR relaxation or by petrophysical laboratory experiments (e.g., triple weighing). The original SDR equation considers the log-mean relaxation time T_{2lm} as a proxy for the pore radius. A linear relationship between r_{eff} and the log-mean relaxation time is expected. We recognize from the graphs in Figure 1 that only the samples of the Araba Formation indicate a nearly linear relationship with a power law exponent 0.956. The slope in the double logarithmic plot is considerably smaller for the samples of the Shahejie Formation. The situation becomes even worse for the Nubia Formation with a negative slope and a coefficient of determination $R^2 = 0.169$.

The weighted harmonic mean T_{2hm} can be used as an alternative proxy for the pore radius. A look at Figure 2 indicates only slight changes. A nearly linear relationship between r_{eff} and T_{2hm} is found for the Araba Formation. The samples of the Nubia formation indicate a weak positive slope. The weighted arithmetic mean T_{2am} indicates similar relationships with weak correlations. The maxima T_{2peak} show a more or less linear relationship with r_{eff} for all three formations with $R^2 > 0.73$ for the Shahejie and Araba Formations but a low value for the Nubia Formation ($R^2 = 0.25$).

The transformation of characteristic relaxation time into a characteristic pore radius uses equation 10 with an individual value of surface relaxivity for each sample. The algorithm of ρ-determination requires an additional expense to get the specific surface area per unit pore volume S_{por}. Considering a wide variation in S_{por} for the samples of a single formation, we get a similar variation in ρ. The graphs in Figure 3 confirm linear relationships between r_{eff} and the characteristic pore radii r_{lm} for the samples of Shahejie and Araba Formations. The situation improves if r_{lm} is replaced by r_{hm}. The resulting graphs in Figure 4 present linear relationships with coefficients of determination $R^2 > 0.79$ for all sandstone formations. The factors of the linear relationship vary in a narrow range between 0.428 and 0.688. Therefore, the characteristic pore radius r_{hm} proves to be a reliable proxy for r_{eff} with a linear relationship $r_{hm} = c\ r_{eff}$. The factor $c = 0.528$ has been determined considering all samples of the three formations. The harmonic mean attributes more weight to the smaller pores or to the pore throats that control the fluid flow. This might be a possible explanation why r_{hm} proves to be a better proxy of r_{eff} in comparison with r_{lm}.

The permeability prediction based on the original SDR equation 6 with $\overline{T_2} = T_{2lm}$ provides only limited predictive quality if a constant prefactor a_1 is used for all sandstone formations. As shown in Figure 5, the permeability prediction works well for the samples of the Shahejie Formation, whereas the SDR equation overestimates k for most samples of the Araba Formation and underestimates k for some samples of the Nubia Formation. An improvement can be achieved if separate prefactors a_1 are determined for each formation (see Figure 6). The variation in the prefactors is related to the average values of surface relaxivity. We get the lowest prefactor with $a_1 = 1.33 \cdot 10^{-9}$ m²/s² for the Araba Formation, which is characterized by a low average surface relaxivity ($\rho = 9.7$ µm/s), and the highest prefactor with $a_1 = 144 \cdot 10^{-9}$ m²/s² for the Nubia Formation with a higher average surface relaxivity ($\rho = 140$ µm/s). The wide variation in the prefactor a_1 underlines the significance of ρ in permeability prediction with the original SDR equation.

We included other characteristic relaxation times in our study. As summarized in Table 1, the use of T_{peak} causes the largest values of the average deviation d and consequently the lowest predictive quality for all considered

sandstone formations. The weighted harmonic mean T_{hm} proves to be advantageous for the Nubia Formation, whereas the weighted arithmetic mean T_{am} results in the lowest d for the Araba Formation.

The direct use of a characteristic pore radius in equation 4 improves considerably the permeability prediction for all sandstone formations. The weighted harmonic mean of pore radii r_{hm}, which proves to be the best proxy for the r_{eff}, enables a high quality permeability prediction with average deviations $d \leq 0.25$ for all considered formations. The porosity exponent $b = 2$ is in good agreement with the theoretical model of equation 4 with $m = 2$. The prefactors a that have been adjusted for the single formations vary only in a narrow range between 0.65 and 1.03. The application of a mean value of the prefactor a provides a reliable predictive quality without any adjustment procedure. However, the better predictive quality can only be achieved if reliable values of surface relaxivity are available for the individual samples. The results of this study confirm the suitability of the approach of ρ-determination as proposed in [2].

6 Conclusions

Three sets of sandstone samples from China and Egypt with a variation of permeability over four orders of magnitude have been selected for the evaluation of the original and modified SDR equations. Our study confirms the applicability of the SDR equation for permeability prediction with the porosity raised to the 4th power. The use of T_{2lm} in the SDR equation has proved to be an appropriate choice. The prefactor in the SDR equation largely depends on the surface relaxivity. Therefore, a calibration procedure has to be applied to adjust the prefactor for a certain lithology.

We modified the SDR equation by replacing the characteristic relaxation time by a characteristic pore radius. The modified equations enable an improved predictive quality. The best results are achieved with weighted harmonic mean r_{hm} that proves to be a reliable proxy for the effective hydraulic radius r_{eff}. However, the transformation of relaxation time into pore radius requires the knowledge of the specific surface area for each sample to determine an individual value of surface relaxivity.

We confirm the potential of the SDR equation in NMR applications. A careful calibration of the equation with suitable values for the prefactor and exponents will contribute to an improved permeability prediction.

Acknowledgements

The authors would like to thank M. Kassab (Egyptian Pertroleum Research Institute) for providing the sandstone samples of the Araba and Nubia Formations and contributing to the petrophysical measurements.

References

1. K. R. Brownstein, C. E. Tarr, Importance of classical diffusion in NMR studies of water in biological cells: Physical Review A, **19**, 2446–2453, doi: 10.1103/PhysRevA.19.2446 (1979).
2. Z. Zhang, A. Weller, Estimating the nuclear magnetic resonance surface relaxivity of Eocene sandstones: A comparison of different approaches: Geophysics, **86**, 2, JM11-JM22, doi: 10.1190/GEO2020-0501.1 (2021a).
3. H. Pape, L. Riepe, J. R. Schopper, A pigeon-hole model for relating permeability to specific surface: The Log Analyst, **23**, 5–13 (1982).
4. Z. Zhang, A. Weller, A comparative study of permeability prediction for Eocene sandstones —Part 1: Application of modified Swanson models to mercury injection capillary pressure and nuclear magnetic resonance data: Geophysics, 86, 6, M233-M243, doi: 10.1190/GEO2021-0194.1 (2021b).
5. G. E. Archie, The electrical resistivity log as an aid in determining some reservoir characteristics: Transactions of American Institute of Mineralogists Metallurgists and Petroleum Engineers, **146**, 54-62 (1942).
6. J. H. Schön, *Physical properties of rocks: A workbook* (Elsevier, 2011).
7. G. Towle, An analysis of the formation resistivity factor-porosity relationship of some assumed pore geometries: Paper C presented at third annual meeting of SPWLA, Houston (1962).
8. A. Weller, L. Slater, Permeability estimation from induced polarization: an evaluation of geophysical length scales using an effective hydraulic radius concept: Near Surface Geophysics, **17**, 581–594, doi: 10.1002/nsg.12071 (2019).
9. R. L. Kleinberg, Utility of NMR T2 distributions, connection with capillary pressure, clay effect, and determination of the surface relaxivity parameter, ρ2: Magnetic Resonance Imaging, **14**, no. 7–8, 761–7, doi: 10.1016/S0730-725X(96)00161-0 (1996).
10. D. O. Seevers, A nuclear magnetic method for determining the permeability of sandstones, in SPWLA 7th Annual Logging Symposium, edited, p. **14**, Soc. of Petrophys. and Well Log Anal (1966).
11. Z. Zhang, A. Weller, Fractal dimension of pore space geometry of an Eocene sandstone formation: Geophysics, **79**, no. 6, D377-387. doi: 10.1190/GEO2014-0143.1 (2014).
12. M. Kassab, A. Weller, H. Abuseda, Integrated petrographical and petrophysical studies of sandstones from the Araba Formation for reservoir characterization: Arabian Journal of Geosciences, 15:944, doi: 0.1007/s12517-022-10221-3 (2022).
13. A. Weller, M.A. Kassab, W. Debschütz, C.D. Sattler, Permeability prediction of four Egyptian sandstone formations, Arabian Journal of Geosciences, **7**, 5171-5183, doi: 10.1007/s12517-013-1188-7 (2014).
14. API (American Petroleum Institute), Recommended Practices for Core Analysis, *API Recommended Practice 40, chapter 6 – permeability determination, second edition*, (1998).

15. A. Weller, L. Slater, A. Binley, S. Nordsiek, S. Xu, Permeability prediction based on induced polarization: Insights from measurements on sandstone and unconsolidated samples spanning a wide permeability range: Geophysics, **80**, 2, D161-D173, doi:10.1190/GEO2014-0368.1 (2015).
16. J. Robinson, L. Slater, A. Weller, K. Keating, T. Robinson, C. Rose, and B. Parker, On permeability prediction from complex conductivity measurements using polarization magnitude and relaxation time: Water Resources Research, **54**, 3436-3452, doi: 10.1002/2017WR022034 (2018).